Received: 12 September 2019 | Revised: 27 December 2019 | Accepted: 27 December 2019

DOI: 10.1096/fj.201902345RR

RESEARCH ARTICLE

THE FASEB JOURNAL

Nuclear accumulation of β-catenin is associated with endosomal sequestration of the destruction complex and increased activation of Rab5 in oral dysplasia

Montserrat Reyes[1,2,3] | **Daniel Peña-Oyarzún**[1,2] | **Patricio Silva**[1,2] | **Sebastián Venegas**[1,2] | **Alfredo Criollo**[1,2] | **Vicente A. Torres**[1,2]

[1]Institute for Research in Dental Sciences, Faculty of Dentistry, Universidad de Chile, Santiago, Chile

[2]Advanced Center for Chronic Diseases (ACCDiS), Universidad de Chile, Santiago, Chile

[3]Department of Pathology and Oral Medicine, Faculty of Dentistry, Universidad de Chile, Santiago, Chile

Correspondence
Vicente A. Torres, Institute for Research in Dental Sciences, Faculty of Dentistry, Universidad de Chile, Calle Sergio Livingstone 943, Independencia, Santiago, Chile.
Email: vatorres@odontologia.uchile.cl

Funding information
Fondo Nacional de Desarrollo Científico y Tecnológico (FONDECYT), Grant/Award Number: 1180495, 1171075 and 3170660; MINEDUC | Comisión Nacional de Investigación Científica y Tecnológica (CONICYT), Grant/Award Number: 15130011

Abstract

Potentially malignant lesions, commonly referred to as dysplasia, are associated with malignant transformation by mechanisms that remain unclear. We recently reported that increased Wnt secretion promotes the nuclear accumulation of β-catenin and expression of target genes in oral dysplasia. However, the mechanisms accounting for nuclear re-localization of β-catenin in oral dysplasia remain unclear. In this study, we show that endosomal sequestration of the β-catenin destruction complex allows nuclear accumulation of β-catenin in oral dysplasia, and that these events depended on the endocytic protein Rab5. Tissue immunofluorescence analysis showed aberrant accumulation of enlarged early endosomes in oral dysplasia biopsies, when compared with healthy oral mucosa. These observations were confirmed in cell culture models, by comparing dysplastic oral keratinocytes (DOK) and non-dysplastic oral keratinocytes (OKF6). Intriguingly, DOK depicted higher levels of active Rab5, a critical regulator of early endosomes, when compared with OKF6. Increased Rab5 activity in DOK was necessary for nuclear localization of β-catenin and Tcf/Lef-dependent transcription, as shown by expression of dominant negative and constitutively active mutants of Rab5, along with immunofluorescence, subcellular fractionation, transcription, and protease protection assays. Mechanistically, elevated Rab5 activity in DOK accounted for endosomal sequestration of components of the destruction complex, including GSK3β, Axin, and adenomatous polyposis coli (APC), as observed in Rab5 dominant negative experiments. In agreement with these in vitro observations, tissue immunofluorescence analysis showed increased co-localization of GSK3β, APC, and Axin, with early endosome antigen 1- and Rab5-positive early endosomes in clinical samples of oral dysplasia. Collectively, these data indicate that increased Rab5 activity and endosomal sequestration of the β-catenin destruction complex leads to stabilization and nuclear accumulation of β-catenin in oral dysplasia.

KEYWORDS

cell signaling, destruction complex, endosome, keratinocyte, oral cancer, oral dysplasia, Rab5, β-catenin

Abbreviations: APC, adenomatous polyposis coli; BSA, bovine serum albumin; DOK, dysplastic oral keratinocyte; EEA1, early endosome antigen 1; GEF, guanine nucleotide exchange factor; GFP, green fluorescent protein; GSK3β, glycogen synthase kinase 3β; GST, glutathione-S-transferase; OSCC, oral squamous cell carcinoma; PBS, phosphate-buffered saline; R5BD, Rab5-binding domain.

1 | INTRODUCTION

Potentially malignant lesions in the oral mucosa are commonly defined, on an histological basis, as oral dysplasia[1,2] and are associated with high rates of progression toward oral squamous cell carcinoma (OSCC).[3,4] Despite the relevance of these lesions, the rates of progression from oral dysplasia toward invasive cancer remain disparate, which is due, in part to the complexity of histopathological diagnosis, and, because no specific markers are available for assuring the evolution of oral dysplasia.[5,6] In this regard, limiting knowledge is available about the molecular alterations involved in the onset and evolution of these lesions,[7,8] and a few signaling molecules have been shown to be deregulated in oral dysplasia. Specifically, it has been shown that components of the Wnt/β-catenin signaling pathway are upregulated in mild and severe oral dysplasia.[9-11] Accordingly, recent studies from our laboratory showed that increased Wnt3a secretion in oral dysplasia leads to nuclear accumulation of β-catenin and Tcf/Lef-dependent transcription of target genes upregulated in oral dysplasia, as shown in patient biopsies and in cell culture models, using dysplastic oral keratinocytes (DOK) and primary cultures of non-tumor oral keratinocytes.[12] Nevertheless, the mechanisms involved in nuclear translocation of β-catenin in oral dysplasia remain unclear.

Early studies showed that Wnt signaling requires the internalization of receptor complexes, and that endosomal localization of components of the β-catenin destruction complex, including Axin and GSK3β, is necessary for nuclear localization of β-catenin.[13,14] Specifically, Wnt3a promotes sequestration of GSK3β within multivesicular bodies, preventing phosphorylation of β-catenin, and thereby increasing nuclear translocation of β-catenin.[13] Indeed, GSK3β has been detected at early and late endosomes,[13] whereas Axin was shown to co-localize with early endosome antigen 1 (EEA1)-positive early endosomes upon Wnt signaling.[14] Once in the nucleus, β-catenin functions as co-activator of Tcf/Lef transcription factors, promoting the expression target genes involved in cell proliferation, viability, migration, and invasion, among other events.[15] Although the mechanisms leading to the endosomal sequestration of the destruction complex have been studied, the identity of endosomal proteins controlling this phenomenon is not completely understood,[16] and most importantly, whether this mechanism is deregulated in premalignant and tumor cells, has not been explored. This is intriguing, because several components and regulators of the endocytic machinery have been shown to undergo either gain or loss of function in different cancers, including OSCC.[17-21] Specifically, within the family of Rab GTPases, which control endocytic trafficking, Rab5 has been reported to be upregulated in different cancers, including lung adenocarcinoma,[22] pancreatic cancer,[23] ovarian cancer,[24] hepatocellular carcinoma,[25] and OSCC.[18]

Rab5 is a small GTPase that controls early endosome dynamics,[26] which has been shown by us and others, to promote the acquisition of different malignant traits, including cell migration and invasion,[27-30] the epithelial to mesenchymal transition,[23] tumorigenesis in vivo,[31] and metastasis in vivo.[27,30] Intriguingly, Rab5 was recently shown to be upregulated in OSCC and associated with malignant traits in this malignancy,[18] however several issues emerge from these findings. First, active Rab5 (ie, GTP-bound), rather than total Rab5 expression, is relevant to promote the acquisition of malignant traits.[28,30,32] Second, unlike those findings reported in OSCC,[18] no evidence is available regarding the expression and/or activation status of Rab5 in potentially malignant lesions, namely oral dysplasia. Third, the functional consequences of any putative alteration of Rab5 in oral dysplasia, have not been explored. The latter is important, based on the ability of Rab5 to control early endosome dynamics, which may impinge in the acquisition of malignant traits in tumor cells, and most importantly, in oral dysplasia. In this context, the accumulation of nuclear β-catenin in tumor cells[15,33,34] and in oral dysplasia[9,10,12] is striking, since these phenomena could be due to increased endosomal targeting of the β-catenin destruction complex. Here, we explored whether endosomal sequestration of the destruction complex accounts for increased accumulation of nuclear β-catenin in oral dysplasia and assessed the role of the endocytic protein, Rab5, in these events. We observed augmented endosomal sequestration of the β-catenin destruction complex in oral dysplasia biopsies and in cultures of dysplastic keratinocytes, when compared with healthy mucosal biopsies and normal keratinocytes, respectively. These events were associated with increased Rab5 activity, and interference with Rab5 activation precluded endosomal sequestration of the destruction complex, decreasing nuclear β-catenin levels and Tcf/Lef-dependent transcription. Taken together, these findings report for the first time, that upregulation of a small GTPase, known to promote the acquisition of malignant traits, contributes with the progression from early oral lesions toward malignant cancer.

2 | MATERIALS AND METHODS

2.1 | Materials

Monoclonal mouse anti-β-catenin (M3539) was from DAKO (DAKO, USA), rabbit monoclonal non-phosphorylated β-catenin Ser33/37/Thr41 (88145) was from Cell Signaling Technology and mouse monoclonal anti-GSK3β (610201) was from BD Transduction Laboratories. Monoclonal antibodies raised against adenomatous polyposis coli (APC)

(sc-9998), Axin (sc-293190), Rab5 (sc-46692), Rab7 (sc-376362), Rab11 (sc-166912), Rabaptin5 (sc-271069), Cyclin D1 (sc-246), Survivin (sc-17779), and GAPDH (sc-365062), as well as polyclonal anti-EEA1 (sc-33585), were from Santa Cruz Biotechnology (Santa Cruz, CA). Alexa Fluor 488, Alexa Fluor 568, and Alexa Fluor 350, conjugated secondary antibodies were from Invitrogen (Carlsbad, CA). Goat anti-rabbit and goat anti-mouse antibodies coupled to horseradish peroxidase (HRP) were from Bio-Rad Laboratories (Hercules, CA). Tissue culture medium, antibiotics and fetal bovine serum (FBS) were from Corning Mediatech. The EZ-ECL chemiluminescent substrate was from Pierce Chemical (Rockford, IL).

2.2 | Cell culture

DOK were obtained from Sigma-Aldrich and maintained in DMEM-high glucose, supplemented with penicillin (10 000 U/mL) and streptomycin (10 µg/mL), 20% Fetal Bovine Serum, and 5 µg/mL Hydrocortisone. The oral keratinocyte cell line, OKF6/TERT2 was kindly donated by Dr Denisse Bravo (Universidad de Chile), and cultured in K-SFM medium containing penicillin (10 000 U/mL) and streptomycin (10 µg/mL) and supplemented with bovine pituitary extract and recombinant human epidermal growth factor (both contained as the K-SFM kit), plus 0.3 mM $CaCl_2$. All cells were incubated at 37°C and 5% CO2. Transfection with the pEGFP-C1 constructs encoding for wild-type Rab5, Rab5/S34N (GDP-bound mutant), and Rab5/Q79L (GTPase deficient mutant), was previously described.[28] Primary cultures of oral keratinocytes were obtained and characterized as previously described.[12] Briefly, tissues were obtained from healthy human oral mucosa of nonsmoking donor subjects (upon previous signature of informed consents, Medical Ethics Committee, Faculty of Dentistry, Universidad de Chile). Tissues were treated with trypsin (0.25%), disintegrated and cultured in K-SFM containing penicillin (10 000 U/mL) and streptomycin (10 µg/mL), and supplemented with bovine pituitary extract and recombinant human epidermal growth factor, plus 0.3mM $CaCl_2$. Fibroblasts were routinely removed by trypsinization.

2.3 | Immunofluorescence

Cells were grown for 24 hours on glass coverslips and following each treatment, samples were fixed with 4% formaldehyde in PBS for 15 minutes, permeabilized with 0.1% Triton X-100/PBS for 15 minutes, washed with PBS, and blocked with 5% bovine serum albumin (BSA)/PBS. Samples were then incubated with primary antibodies overnight at 4°C, washed three times (PBS, 5 minutes) and incubated with secondary antibodies for 1 hour, and then washed three times and mounted using the DAKO assembly medium. The samples were visualized by microscopy, using a Nikon C2 Plus confocal microscope.

2.4 | Tissue immunofluorescence

This study was approved by the Ethical Committee from the Faculty of Dentistry. Biopsy sections (3 µm, paraffin blocks) were obtained from 30 patients diagnosed with mild or moderate/severe dysplasia at ratios 50% and 50%, as informed by the oral pathologist in sections previously stained with hematoxylin and eosin. Also, three healthy patient samples were included in this study. Paraffin blocks were deparaffinized in xylol and rehydrated in decreasing alcohol, for antigenic recovery. Samples were permeabilized with 0.3% Triton X-100/PBS for 15 minutes, washed twice, and then incubated with 5% BSA for 30 minutes. Samples were then incubated with primary antibodies overnight at 4°C, followed by incubation with secondary antibodies for 1 hour and subsequently mounted with DAKO. Samples were visualized by confocal microscopy (Nikon C2 Plus).

2.5 | Subcellular fractionation

Cells were washed twice with ice-cold PBS and homogenized in fractionation buffer supplemented with protease inhibitors and phosphatases. The cell homogenate was shaken at 30-50 rpm, for 30 minutes at 4°C. Subsequently, samples were centrifuged at 720g, 4°C for 5 minutes. The pellet was separated from the supernatant, to obtain nuclear and cytoplasmic proteins. Pellet was then washed with fractionation buffer and centrifuged at 720 g, 4°C for 10 minutes, removing the supernatant, and resuspending the pellet in lysis buffer.

2.6 | β-catenin Tcf/Lef reporter assay

For Tcf/Lef transcriptional activity measurements, the luciferase reporter activity system was used, as previously described.[12] This assay is based on transfection with the plasmids pTOP-FLASH, which encodes for the luciferase gene preceded by three tandem Tcf/Lef binding sites, and the pFOP-FLASH, which contains point mutations on these sites. The constitutively active vector encoding for Renilla luciferase (Promega, Madison, WI, USA) was used as co-transfection control. Cells were transfected with 1.5 µg of each plasmid for 24 hours, and then cells were homogenized in a buffer containing 0.1 M KH_2PO_4 (pH 7.9), 1 mM DTT, 0.5% Triton X-100. Then, 50 µL of KTME buffer (100 mM Tris HCl pH 7.8, 10 mM $MgSO_4$, 2 mM EDTA) was added, containing

the substrates luciferin (0.073 mM) and ATP (5.5 μM). The luciferase activity was quantified in a luminometer.

2.7 | Rab5-GTP, Rab7-GTP, and Rab11-GTP pulldown assays

Rab5-GTP, Rab7-GTP, and Rab11-GTP pulldown assays were performed as previously described.[35] Briefly, cells were lysed in a buffer containing 25 mM HEPES (pH 7.4), 100 mM NaCl, 5 mM $MgCl_2$, 1% NP 40, 10% glycerol, 1 mM dithiothreitol, and protease inhibitors. Extracts were incubated for 5 minutes on ice and clarified by centrifugation (10 000 *g*, 1 minutes, 4°C). Post-nuclear supernatants (95% of homogenate) were immediately used for pulldown assay, in order to avoid GTP hydrolysis, while remnant supernatants (5% of homogenate) were used for input analysis of Rab5, Rab7, or Rab11 (note that no total Rab protein could be normalized with loading control or total protein content, since this method is not adequate for whole cell lysate analysis). Pulldown assays were performed with 30 μg of GSH beads precoated with GST-R5BD (Rab5-GTP pulldown), GST-RILP (Rab7-GTP pulldown), or GST-FIP (Rab11-GTP pulldown), per condition. Beads were incubated with supernatant for 15 minutes at 4°C in a rotating shaker. Thereafter, beads were collected, washed with lysis buffer containing 0.01% NP 40 and samples were analyzed by Western blotting.

2.8 | SDS-PAGE and Western blot

Cells were washed with ice-cold PBS and homogenized in lysis buffer supplemented with protease and phosphatase inhibitors. Subsequently, the total protein extracts were subjected to denaturing polyacrylamide gel electrophoresis (SDS-PAGE). Resolved proteins were transferred to nitrocellulose membranes and used for Western blotting. Membranes were blocked with 5% fish skin gelatin in 0.1% Tween-TBS and then incubated with antibodies. Primary antibodies were detected with secondary antibodies conjugated with the enzyme HRP and determined by using the chemiluminescence EZ-ECL system.

2.9 | Protease protection assay

Protease protection assays were performed as previously described.[13,36] Cells were harvested from 10 cm plates, collected by centrifugation at 4°C, and then resuspended in buffer (100 mM potassium phosphate pH 6.7, 5 mM $MgCl_2$, 250 mM sucrose) containing 6.5 mg/mL digitonin, incubating them for 5 minutes at room temperature, followed by 30 minutes on ice. Digitonin solution was removed by centrifugation at 13 000 rpm (5 minutes) in an Eppendorf centrifuge. Permeabilized cells were resuspended in buffer without digitonin and aliquoted into eppendorf tubes containing stocks of reagents that will generate final concentrations of 1 mg/mL Proteinase K, 1 mg/mL Proteinase K with 0.1% Triton X-100, or nanopure water. Samples were incubated for 10 minutes at room temperature and the reaction was stopped by the addition of pre-heated loading buffer containing 20 mM PMSF, followed by an additional heating at 95°C (5 minutes). Samples were analyzed by SDS-PAGE and Western blotting.

2.10 | Statistical analysis

An exploratory data analysis were performed using descriptive statistics. T test and ANOVA were used. Values averaged from at least three independent experiments were compared. A value of significance of 5% or less ($P < .05$) was accepted as statistically significant. All statistical tests were performed using Stata 11.0 software.

3 | RESULTS

3.1 | Enlarged early endosomes and increased Rab5 activity in oral dysplasia

Altered endosome dynamics and aberrant endosome size have been reported in tumor cells in vitro; however, functional consequences of these alterations in early premalignant lesions have not been assessed, and most importantly, whether these alterations are observed in clinical samples remain unexplored. To evaluate these possibilities, we assessed early endosomal structures in potentially malignant lesions of the oral mucosa, specifically oral dysplasia samples with different grading (Figure S1). In doing so, tissue immunofluorescence assays showed that early endosomes are substantially enlarged in oral dysplasia biopsies, when compared with healthy oral mucosa, as shown by immunofluorescence staining against the early endosome marker, EEA1 (Figure 1A). Specifically, severe oral dysplasia and, to a lesser extent, mild dysplasia samples, showed substantial increases in early endosome size, when compared with healthy oral mucosa (Figure 1B). These observations were confirmed in vitro, by comparing dysplastic (DOK) and non-dysplastic (OKF6) oral keratinocytes, since DOK depicted increased number of EEA1-positive particles ranging between 0.05-0.5 μm^2 and 0.5-2 μm^2 (Figure 1C). Similar results were observed with another marker of early endosomes, Rabaptin5, which showed higher accumulation of intermediate-sized particles in DOK (Figure 1D). Remarkably, Rab5, which is a marker of different structures, including early endosomes and endocytic vesicles, showed a modest, but non-significant increase

of particles ranging between 0.5-2 μm^2, when comparing OKF and DOK (Figure 2A,B). This could be, because, unlike EEA1 and Rabaptin5, Rab5 immunodetection does not discriminate between active or total Rab5. As for Rab5, staining of Rab7 and Rab11, which are markers routinely used for detecting late and recycling endosomes, respectively, showed no significant changes in the population of intermediate or large structures (Figure 2A,B). In addition, Rab7 signal intensity appeared slightly increased in DOK (Figure 2A), but differences were not significant.

The observation that early endosomes are enlarged in oral dysplasia, as judged with two effectors of active GTP-bound Rab5 (EEA1 and Rabaptin5), but not with total Rab5, is intriguing, since the activation status of Rab5 represents

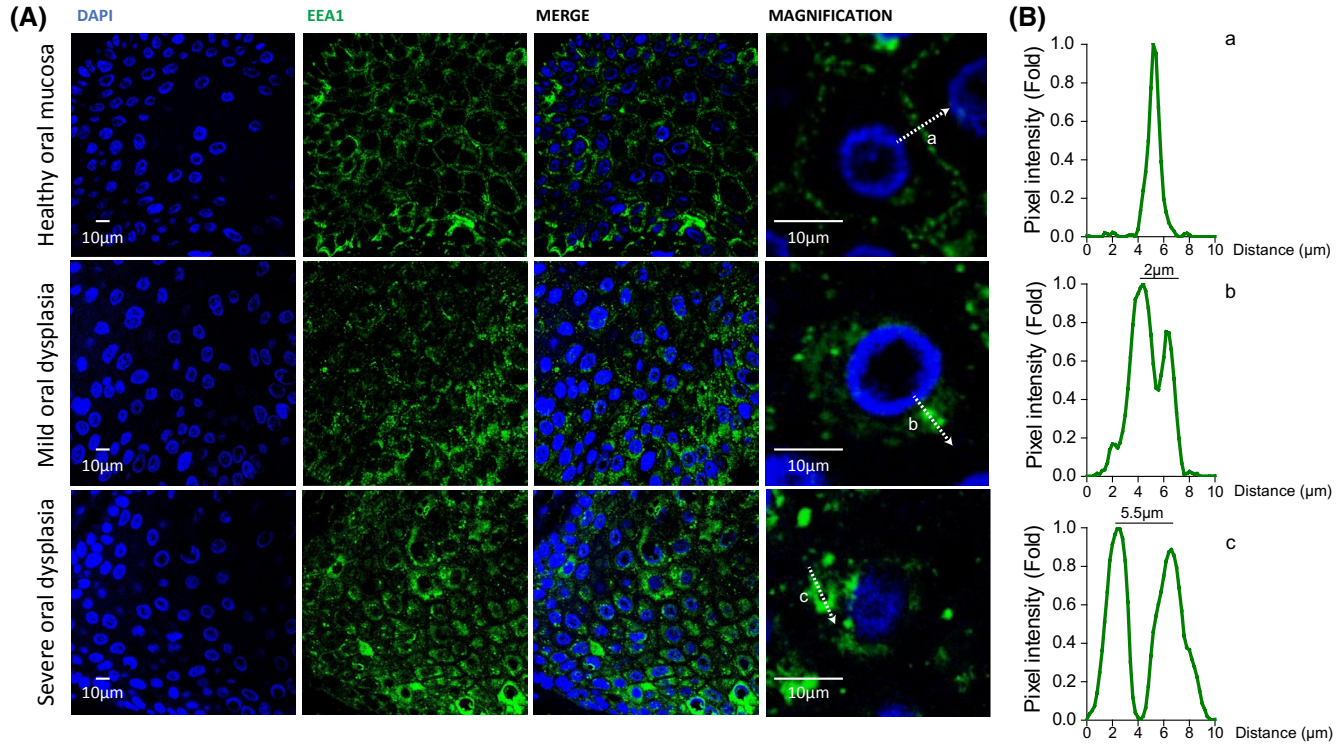

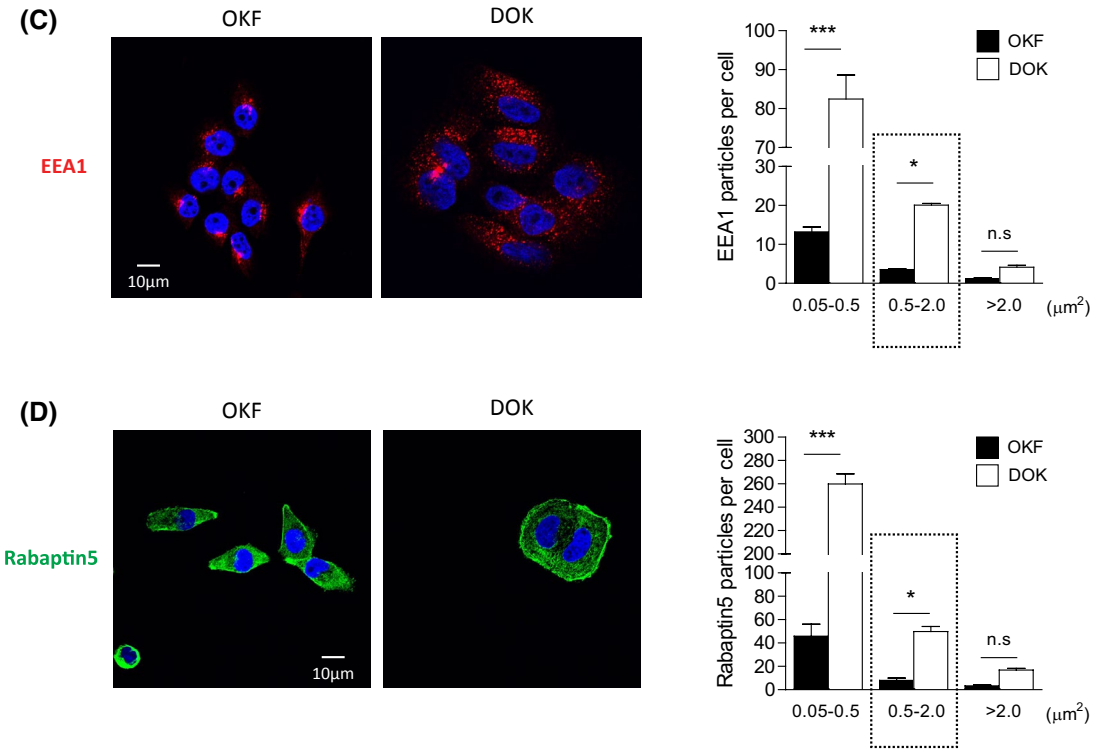

FIGURE 1 Enlarged early endosomes in oral dysplasia. A, Tissue immunofluorescence for early endosome detection in clinical samples of severe oral dysplasia and healthy oral mucosa. Early endosomes were visualized by immunofluorescence, using a monoclonal antibody raised against the early endosome antigen 1 (EEA1) marker, whereas nuclei were stained with DAPI. Images were captured by confocal microscopy, using a 60× magnification and are representative from three different cases of oral dysplasia and healthy oral mucosa. Bar represents 10 μm. B, Endosome diameter was obtained from images described as in (A), by measuring the pixels distributed on a line drawn across vesicles (shown in the right panels). All lines were equally sized and representative graph profiles are shown. Length in microns is shown in the *x*-axis. C, Dysplastic (DOK) and non-dysplastic OKF6/Tert2 (OKF6) oral keratinocytes were grown in coverslips, fixed, and stained with antibodies raised against EEA1, whereas nuclei were visualized with DAPI. Representative confocal microscope images are shown. Bar represents 10 μm. EEA1-positive particle size and amount were analyzed with the Image J software. According to their size, particles were grouped in three categories, 0.05-0.5, 0.5-2.0 and >2.0 μm^2. The graph represents the analysis of at least 500 cells pooled from three independent experiments, and data are plotted as the number of particles within those categories (mean ± SEM; $*P \leq .05$; $***P \leq .001$; n.s., non-significant). D, Rabaptin5-positive particles were analyzed as described in (C). Representative confocal images are shown (bar represents 10 μm). The graph represents size distribution of particles, which were grouped in the same categories described in (C). Data were obtained from at least 500 cells pooled from three independent experiments (mean ± SEM; $*P \leq .05$; n.s., non-significant)

an important point of control in early endosome dynamics.[26] In this context, the role and activity of Rab5 and other Rab GTPases has not been explored in premalignant lesions and OSCC. By using a pulldown assay,[28,35,37] we measured Rab5-GTP levels in cultures of DOK and OKF6 cells. Intriguingly, DOK cells depicted more than 3-fold increase in Rab5-GTP levels, when compared with OKF6 cells (Figure 2C). Conversely, no fluctuations were observed in the activation status of other related endosomal Rabs, since neither Rab7-GTP nor Rab11-GTP levels differed between OKF6 and DOK cells, as shown by pulldown assays (Figure 2D,E). Collectively, these observations suggest that increased early endosome size in oral dysplasia is associated with augmented activity of Rab5, but not other Rab GTPases.

3.2 | Rab5 activity is required for nuclear accumulation of β-catenin and the expression of target genes upregulated in oral dysplasia, via endosomal sequestration of the destruction complex

The observation that DOK cells depict increased Rab5-GTP levels and larger early endosomes (this study), together with previous evidence showing augmented nuclear β-catenin in oral dysplasia samples and DOK cells,[12] raised the question as to whether augmented Rab5 activity accounts for nuclear accumulation of β-catenin in DOK cells. To address this possibility, Rab5 activity was reduced in DOK cells by using a dominant-negative approach. Specifically, DOK cells were transfected with GFP or GFP-Rab5/S34N (GDP-bound, inactive Rab5 mutant) and the localization of β-catenin was analyzed by immunofluorescence and confocal microscopy. As previously reported,[12] transfection with an empty vector (GFP) did not affect nuclear detection of β-catenin in DOK cells, however, transfection with GFP-Rab5/S34N caused a substantial decrease of nuclear β-catenin (Figures 3A and S2). These observations were further supported by biochemical fractionation, since expression of GFP-Rab5/S34N, but not GFP alone, decreased the enrichment of both total β-catenin and transcriptionally active, non-phosphorylated β-catenin in nuclear fractions (Figure 3B). Given that nuclear accumulation of β-catenin in DOK cells is associated with augmented Tcf/Lef-dependent transcription and expression of β-catenin target genes, such as survivin and cyclin D1,[12] we evaluated the requirement of Rab5 activity in both events. Multiple co-transfections in DOK cells are not feasible, as these proceed with low efficiency and cell viability is impaired (data not shown). Hence, we used an alternative approach, by stimulating OKF6 cells with conditioned medium derived from DOK cells, which was previously shown to contain Wnt ligands, thereby stimulating Wnt/β-catenin signaling and Tcf/Lef-dependent transcription.[12] First, we evaluated the dependency on Wnt3a, by using the compound Wnt-C59, which inhibits secretion of Wnt3a, but not other Wnt ligands in DOK cells.[12] As expected, Wnt-C59 abrogated Tcf/Lef-dependent transcription, induced by DOK-derived conditioned medium in OKF cells (Figure 3C). Thereafter, the requirement of Rab5 activity in Tcf/Lef-dependent transcription was evaluated in OKF6 cells transfected with GFP or GFP-Rab5/S34N, observing that GFP-Rab5/S34N decreased Tcf/Lef-dependent transcription induced by DOK-derived conditioned medium (Figure 3C). In accordance with these observations, transfection of DOK cells with GFP-Rab5/S34N, but not GFP alone, caused a partial decrease in the expression of different β-catenin targets, including survivin and cyclin D1 (Figure 3D). Finally, to evaluate the effects of Rab5 activity in β-catenin-dependent signaling, OKF cells, which harbor low levels of nuclear β-catenin,[12] were transfected with the constitutively active mutant of Rab5 GFP-Rab5/Q79L. In doing so, the sole expression of GFP-Rab5/Q79L, but not GFP alone, was sufficient to promote nuclear re-localization of β-catenin in OKF cells (Figure 3E). Importantly, as previously reported,[12] treatment with conditioned medium obtained from DOK cells (which are known to secrete Wnt3a) promoted nuclear localization of β-catenin

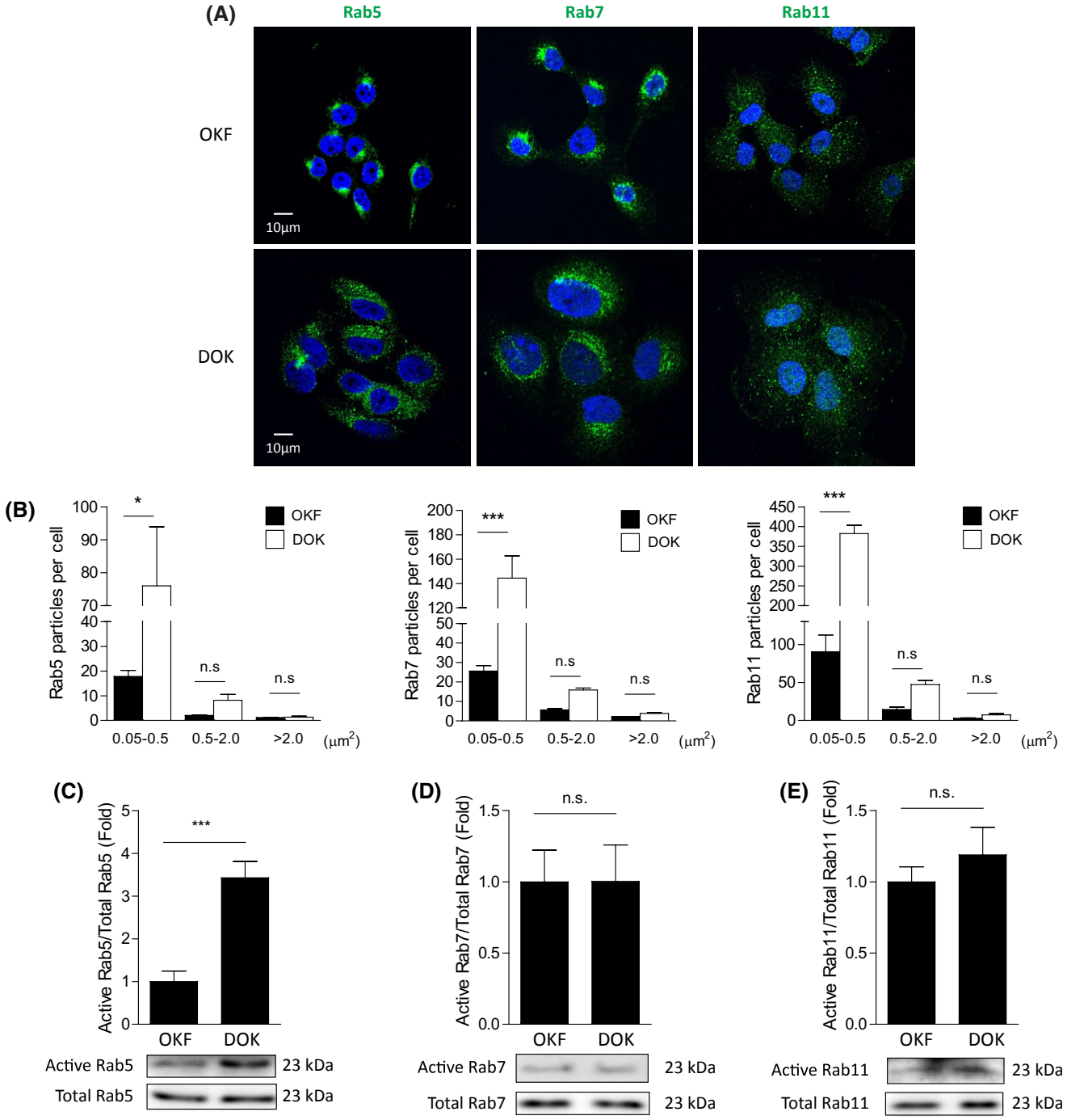

FIGURE 2 Distribution of endosomes and activity of Rab proteins in DOK. A, Dysplastic (DOK) and non-dysplastic OKF6/Tert2 (OKF6) oral keratinocytes were grown in coverslips, fixed, and stained with antibodies raised against Rab5 (early endosomes), Rab7 (late endosomes), or Rab11 (recycling endosomes), whereas nuclei were visualized with DAPI. Representative confocal microscope images are shown. Bar represents 10 µm. B, Rab5-, Rab7- or Rab11-positive particle size and amount were analyzed with the Image J software. According to their size, particles were grouped in three categories, 0.05-0.5, 0.5-2.0 and >2.0 μm^2. Graphs represent the analysis of at least 500 cells pooled from three independent experiments, and data are plotted as the number of particles within those categories (mean ± SEM; ***$P \leq .001$; n.s., non-significant). C, DOK and OKF6 cells were grown for 24 hours and whole cell lysates were prepared. Rab5-GTP levels were determined by the GST-R5BD pull-down assay. Lower panels, representative Western blot images from four independent experiments are shown. Upper graph, relative Rab5-GTP levels normalized to total Rab5 by scanning densitometry are shown as the fold increase with respect to OKF6 cells. Data represent the average of four independent experiments (mean ± SEM). **$P < .01$. D,E, Whole cell lysates were obtained from DOK and OKF6 cells and then, Rab7-GTP and Rab-11-GTP levels were measured in GST-RILP and GST-FIP3 pulldown assays, respectively. Representative Western blot images and relative levels of Rab7-GTP and Rab11-GTP were obtained as described in (C). Data represent the average of five independent experiments (mean ± SEM)

in OKF cells, and this effect was further increased in cells transfected with Rab5/Q79L (Figure 3E). Taken together, these observations indicate that Rab5 activity is required for nuclear localization of β-catenin and transcription of target genes.

To gain insights about the mechanisms whereby Rab5 promotes nuclear localization of β-catenin and downstream events, we evaluated the requirement of Rab5 in the endosomal sequestration of components of the destruction complex in oral dysplasia. To this end, we evaluated GSK3β, APC

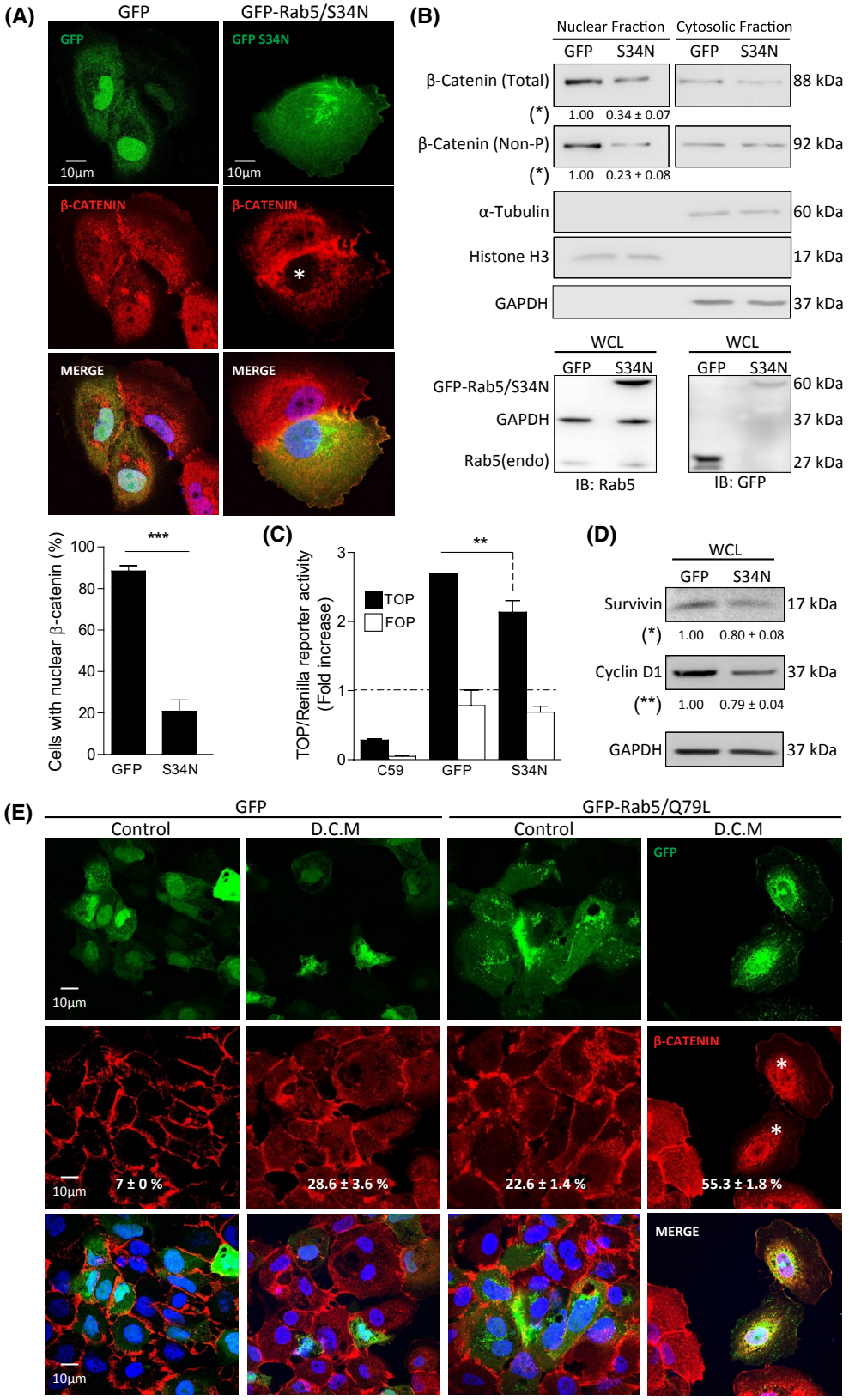

FIGURE 3 Rab5 activity is required for nuclear localization of β-catenin and Tcf/Lef-dependent transcription in DOK. A, DOK cells were transfected with either GFP or GFP-Rab5/S34N for 24 hours, samples were fixed and stained with an antibody against total β-catenin, whereas nuclei were visualized with DAPI. Representative confocal microscope images are shown. Bar represents 10 μm. The graph indicates the percentage of cells with nuclear localization of total β-catenin in GFP-positive cells, obtained as described in the materials and methods, using the Image J software. Data represent the average from three independent experiments (mean ± SEM; *t* test; ***$P \leq .001$). B, Subcellular fractionation of DOK cells was performed as described in the materials and methods. Total and non-phosphorylated β-catenin were evaluated by Western blot, using specific antibodies. Histone H3, α-tubulin, and GAPDH were used as nuclear and cytosolic markers, respectively. Representative images are shown. Numbers below each panel represent the nuclear/cytosolic ratio for total (total) and non-phosphorylated β-catenin (non-P), obtained by scanning densitometry of Western blot images, and shown as the fold change with respect to GFP. Data were averaged from three independent experiments (mean ± SEM). Lower panels correspond to representative images of whole cell lysates (WCL), which were analyzed for total GFP and GFP-Rab5/S34N in homogenates, using specific antibodies against Rab5 and GFP, whereas GAPDH was included as loading control. The efficiency of transfection was determined by cell counting in a fluorescence microscope and corresponded to 50% (GFP) and 45% (GFP-Rab5/S34N). C, OKF6 cells were co-transfected with the plasmids pTOP-FLASH (functional Tcf/Lef binding sites, black bars) or pFOP-FLASH (mutated, non-functional Tcf/Lef binding sites, grey bars), along with GFP alone or GFP-Rab5/S34N. The constitutively active vector encoding for renilla luciferase was used as control. Thereafter, Wnt/β-catenin activity was stimulated in OKF6 cells by incubation with either control medium, conditioned medium obtained from DOK cells, or conditioned medium derived from DOK cells previously treated with the Wnt-C59 inhibitor. After 24 hours, cells were homogenized and prepared for Tcf/Lef reporter assays (see materials and methods for details). Data were obtained as the ratio luciferase/renilla activity and shown as the relative values with respect to control medium-treated cells (adjusted to 1, dashed line in the graph). Data were averaged from three independent experiments (mean ± SEM; *t* test; **$P \leq .01$). D, Western blot analysis of DOK cells transfected with GFP or GFP-Rab5/S34N. Survivin, cyclin D1, GFP, and GAPDH were blotted with specific antibodies. Representative images are shown from three independent experiments. Numbers below panel indicate relative levels of survivin and cyclin D1, which were quantified by scanning densitometry, normalized with respect to GAPDH and shown as the mean ± SEM (*$P \leq .05$ for survivin; **$P \leq .01$ for cyclin D1). E, DOK cells were transfected with GFP or GFP-Rab5/Q79L, treated with either control or DOK conditioned medium and analyzed by confocal microscopy, as described in (A). Representative images are shown (bar, 10 μm). Numbers inside each panel indicate the percentage of cells with nuclear localization of β-catenin in GFP-positive cells, which was obtained by averaging three independent experiments (mean ± SEM; *$P \leq .05$, multiple comparisons)

and Axin by immunofluorescence microscopy, and analyzed their localization with respect to the early endosome-specific marker, EEA1. Of note, all three components rendered cytosolic localization, although Axin showed partial nuclear localization, which is in agreement with early reports (Figure S3).[38] Interestingly, GSK3β, which is responsible of β-catenin phosphorylation, was readily detected at early endosomes in DOK cells, as judged by co-localization with EEA1 (Figure 4A). Nevertheless, transfection with GFP-Rab5/S34N, but not GFP alone, decreased the extent of co-localization between GSK3β and EEA1, suggesting that interference with Rab5 activity impairs the recruitment of GSK3β within early endosomes (Figure 4A). To confirm these observations, we evaluated two additional components of the destruction complex, APC and Axin. In agreement with data obtained for GSK3β, both APC and Axin were detected at early endosomes in DOK cells, and expression of GFP alone did not affect this pattern (Figure 4B,C). Most importantly, expression of GFP-Rab5/S34N decreased the extent of co-localization of both Axin and APC, with EEA1 (Figure 4B,C), further indicating that dominant negative Rab5 interferes with the localization of APC and Axin at early endosomes. Taken together, these observations indicate that components of the β-catenin destruction complex are recruited within early endosomes and that this sequestration depends on functional Rab5.

Since Wnt3a secretion by DOK is responsible of nuclear accumulation of β-catenin[12] and Tcf/Lef-dependent transcription (Figure 3C), we sought to evaluate the requirement of Wnt3a, on endosomal localization of components of the destruction complex. To this end, OKF6 were challenged with conditioned medium obtained from DOK, and co-localization between GSK3β and EEA1 was evaluated in both OKF and primary cultures of oral keratinocytes. In doing so, DOK-derived conditioned medium increased the extent of co-localization between GSK3β and EEA1 in both OKF (Figure 5A) and primary keratinocytes (Figure 5B). Notably, as control, Wnt3a alone evoked the effects of DOK-derived medium in OKF and primary keratinocytes (Figure 5A,B), supporting the notion that Wnt3a produced by DOK is responsible of increased localization of GSK3β at early endosomes.

3.3 | Endosomal localization of components of the β-catenin destruction complex is increased in oral dysplasia biopsies

So far, our observations suggest that the endosomal sequestration of components of the destruction complex is increased in DOK. These observations were also supported in a protease protection assay, which allows evaluating the localization of components within membrane-bounded compartments.[13,36] Here, DOK showed higher protection of GSK3β and Axin against proteinase K, when compared with OKF (Figures 6A,B and S4A), and proteinase K protection depended on Rab5 (Figure S4B), further supporting the notion that the endosomal sequestration of components of the destruction complex

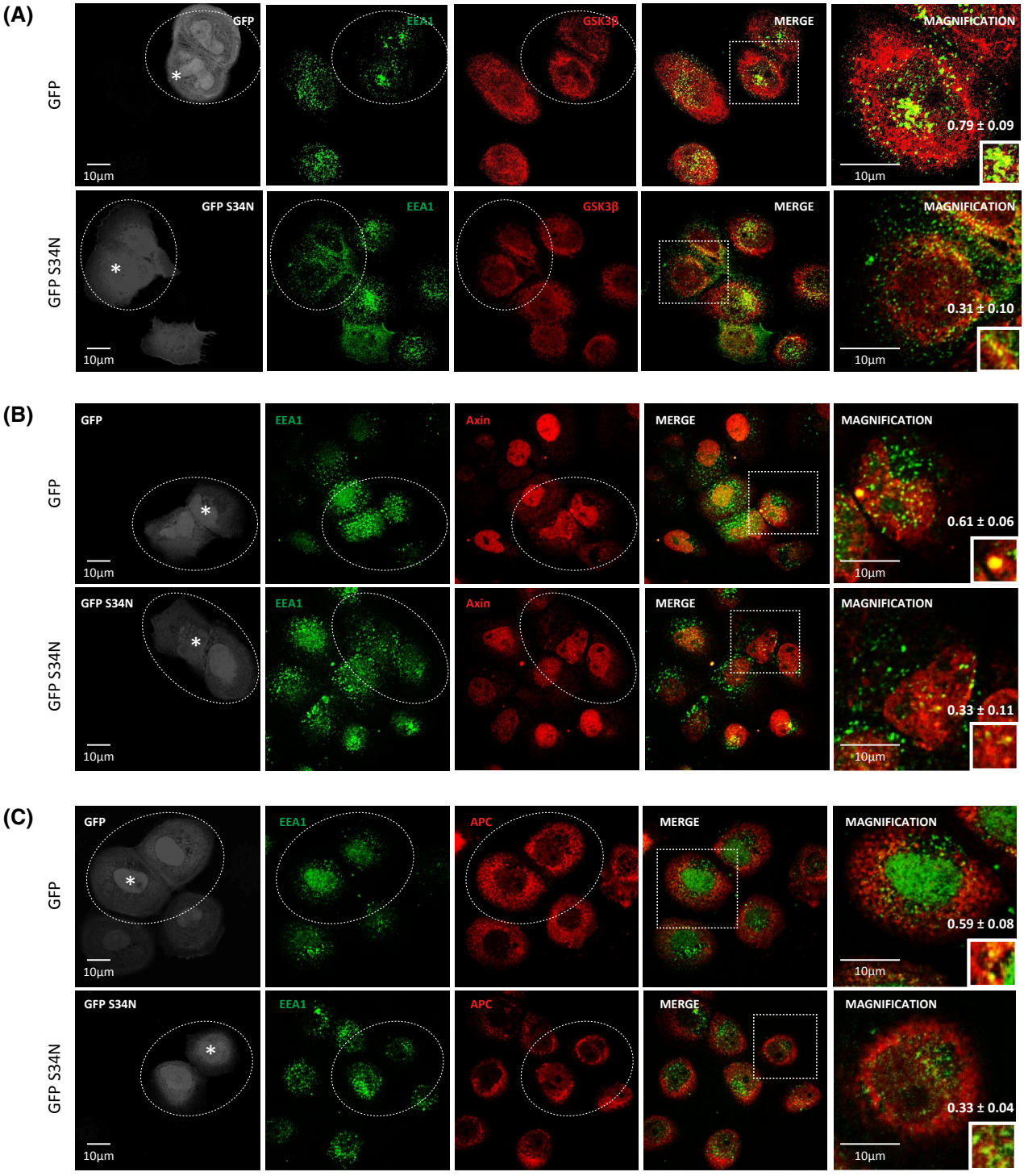

FIGURE 4 Endosomal localization of the β-catenin destruction complex requires Rab5. DOK cells were transfected with either GFP or GFP-Rab5/S34N for 24 hours, samples were fixed and co-stained with antibodies raised against EEA1 and GSK3β (A), EEA1 and Axin (B), or EEA1 and APC (C), followed by fluorescent secondary antibodies Alexa Fluor 568 (GSK3β, Axin, APC) and Alexa Fluor 350 (EEA1). For image representation, GFP- and GFP-Rab5/S34N-positive cells were gated, as shown in the left panels (gray channel), and confocal images were represented for EEA1 (green channel) and GSK3β, Axin or APC (red channel). Representative images are shown in the middle panels. Right panels represent magnifications of boxed areas, as shown. Bar, 10 μm. Numbers inside each panel indicate the Mander's Coefficient, which was obtained for EEA1 and GSK3β (A), EEA1 and Axin (B), or EEA1 and APC (C), and shown as the average of three independent experiments (mean ± SEM; *t* test; $***P \leq .001$ in A, B; $**P \leq .01$ in C)

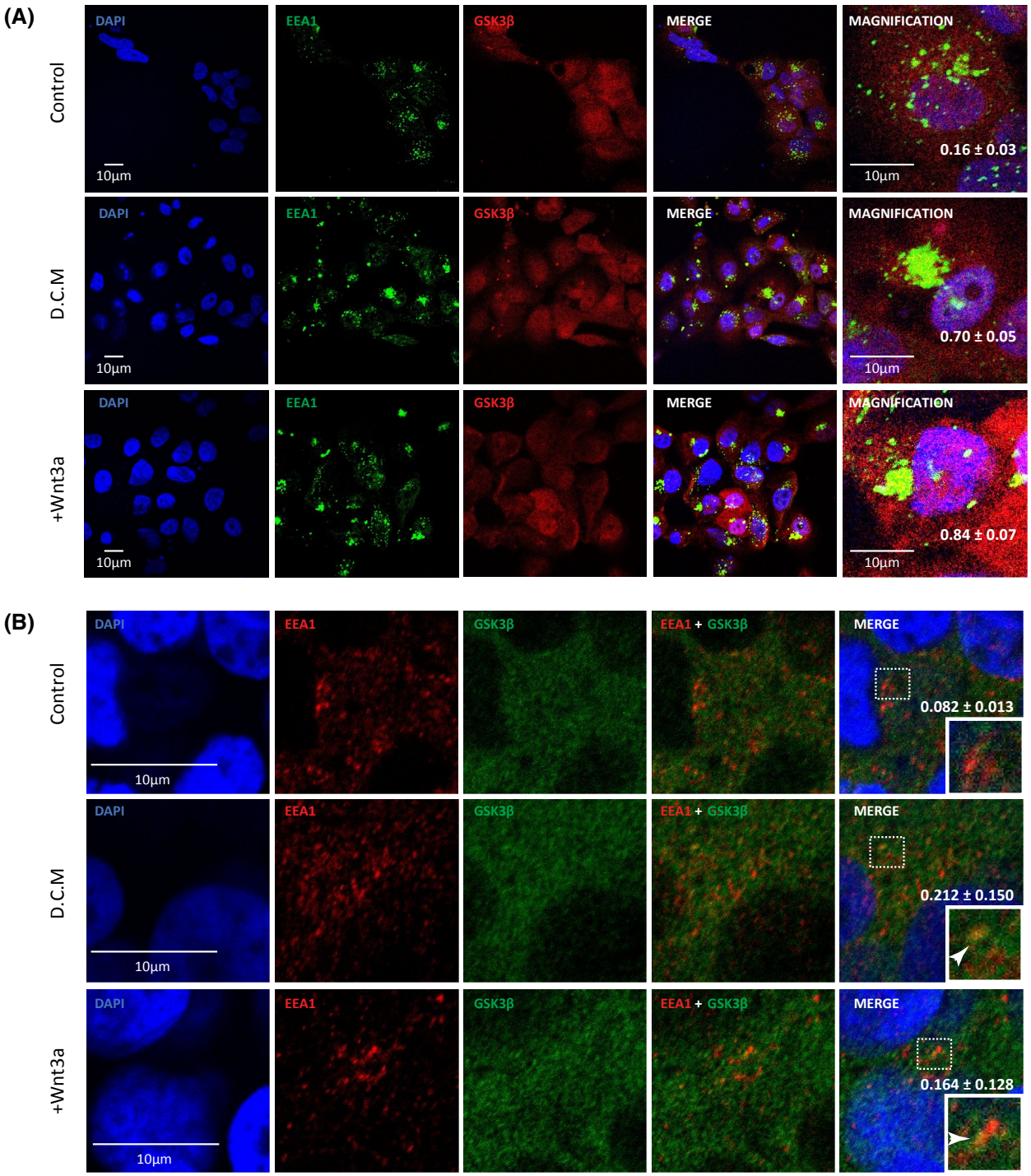

FIGURE 5 Wnt3a promotes endosomal localization of GSK3β in primary and non-dysplastic oral keratinocytes. Non-dysplastic OKF6/Tert2 (OKF6) oral keratinocytes (A) and primary oral keratinocytes obtained from a healthy donor (B) were treated with control medium, DOK conditioned medium or Wnt3a-enriched medium for 24 hours, samples were fixed and co-stained with antibodies raised against EEA1 and GSK3β, followed by fluorescent secondary antibodies Alexa Fluor 568 and Alexa Fluor 488. Nuclei were visualized with DAPI. Representative confocal images are shown. Right panels indicate magnifications of boxed areas, as shown. Bar, 10 μm. Numbers inside each panel indicate the Mander's Coefficient (mean ± SD)

is increased in dysplastic keratinocytes. To evaluate whether these in vitro observations are extended to the clinical level, we analyzed the extent of co-localization between GSK3β and EEA1-positive early endosomes in oral dysplasia biopsies and healthy oral mucosa. Likewise, to establish a correlation between the endosomal sequestration of GSK3β and the nuclear detection of β-catenin in clinical samples, we assessed β-catenin localization by tissue immunofluorescence. First, as previously reported, β-catenin was mostly nuclear in oral dysplasia biopsies, when compared with healthy oral mucosa

(Figure 6C). Thereafter, by serial sections of the same paraffin-embedded tissue, containing nuclear β-catenin, we analyzed the extent of co-localization between GSK3β and EEA1. In agreement with cell culture data, co-localization of GSK3β and EEA1 was higher in severe oral dysplasia and to a lesser extent in mild oral dysplasia biopsies, when compared with healthy oral mucosa samples (Figure 6D-F). Notably, this co-localization pattern was markedly pronounced in regions of the biopsy depicting augmented nuclear β-catenin. These observations were confirmed with alternative markers of early endosomes and components of the destruction complex, including APC (Figure 7A), Axin (Figure 7B), and Rab5 (Figure 7C), since their extent of co-localization was progressively increasing with the different grades of dysplasia. Collectively, these

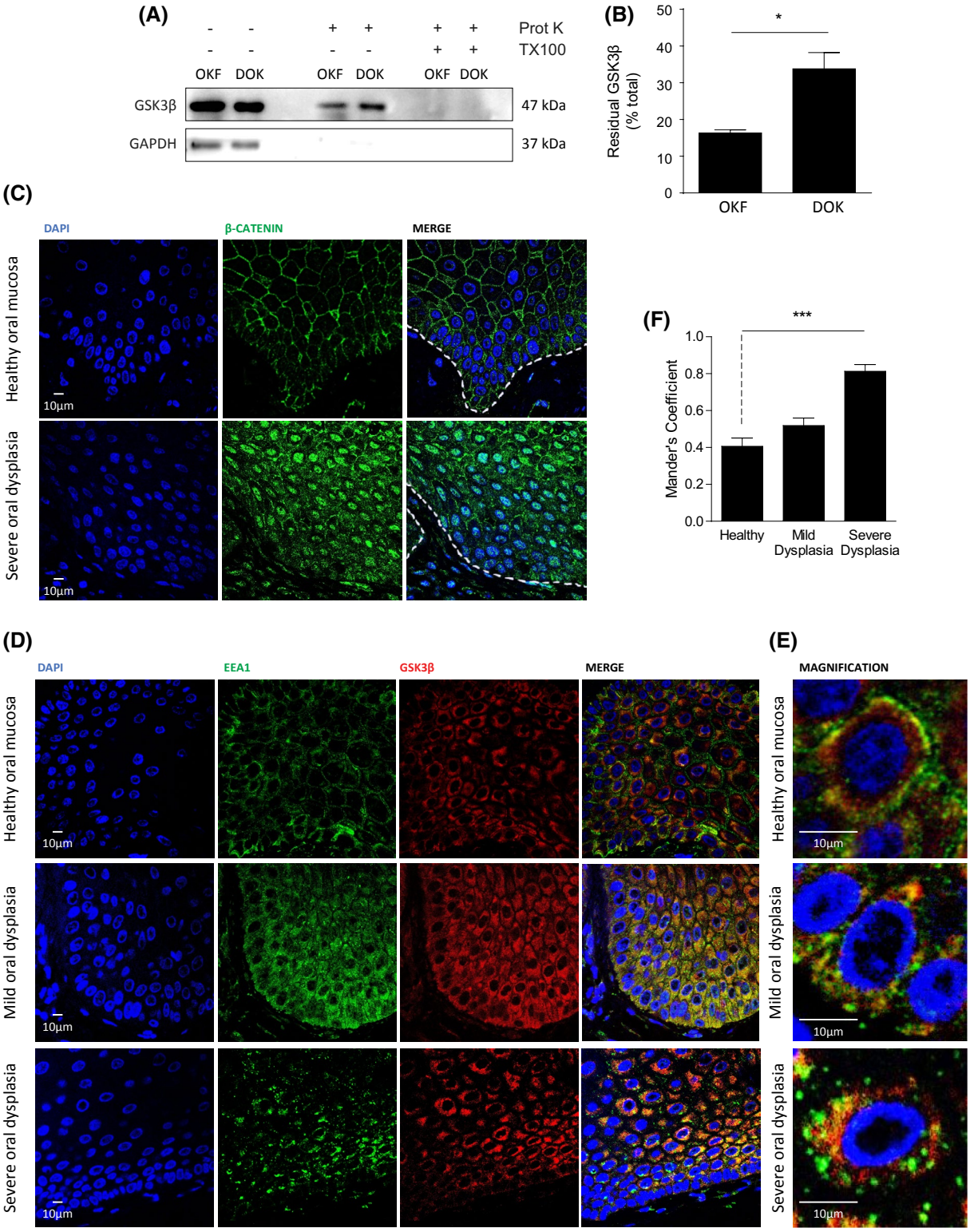

FIGURE 6 Nuclear accumulation of β-catenin is associated with endosomal sequestration of GSK3β in oral dysplasia. A, Protease protection assay. Dysplastic (DOK) and non-dysplastic OKF6/Tert2 (OKF6) oral keratinocytes were cultured for 24 hours, harvested and processed for Proteinase K treatment, as described in the materials and methods. Samples were either left untreated or incubated with Proteinase K or Proteinase K + 0.1% Triton X-100, for 10 minutes. Samples were analyzed by Western blot, using antibodies raised against GSK3β or GAPDH. Representative images are shown. B, Proteinase K-resistant GSK3β was quantified by scanning densitometry and normalized to GSK3β input levels in non-treated samples (% residual GSK3β). The graph represents the average obtained from three independent experiments (mean ± SEM; $*P < .05$). C, Tissue immunofluorescence of β-catenin in healthy oral mucosa and severe oral dysplasia. Formalin fixed paraffin-embedded samples were obtained from the Laboratory of Pathological Anatomy (Faculty of Dentistry, Universidad de Chile) and histologically classified by an oral pathologist. Biopsy sections (3 μm) were deparaffinized in xylol, rehydrated and then permeabilized with 0.3% Triton X-100/PBS for 15 minutes, for subsequent indirect immunofluorescence analysis. β-catenin was detected with a primary antibody, followed by the respective Alexa Fluor-conjugated secondary antibody and mounted for confocal microscopy imaging (Nikon C2 Plus, image capture at 60× magnification). Nuclei were visualized with DAPI. Representative images are shown, and dashed lines indicate the epithelial/connective lining. Bar, 10 μm. D,E, Tissue immunofluorescence of GSK3β and EEA1 was performed in healthy oral mucosa, mild oral dysplasia and severe oral dysplasia biopsies, specifically within the same area and slice depicting nuclear localization of β-catenin, as shown in (A). Nuclei were visualized with DAPI. D, Representative images are shown from three independent experiments. Bar represents 10 μm. E, Representative magnification of boxed areas shown in (D). F, The graph indicates the Mander's Coefficient for EEA1 and GSK3β, and obtained from three independent experiments, by analyzing at least 50 cells per condition, and averaged from all samples (mean ± SEM; $***P \leq .001$)

data indicate that endosomal localization of components of the destruction complex, including GSK3β, Axin and APC, is augmented in oral dysplasia biopsies and that this phenomenon is associated with nuclear accumulation of β-catenin.

4 | DISCUSSION

Aberrant activation of the Wnt/β-catenin pathway is associated with the development and progression of different malignancies,[15,33,34] however, the role that it plays in premalignant lesions has been recently acknowledged. By focusing in oral lesions, we and others have observed that β-catenin is progressively accumulated in the nucleus of dysplastic cells, as shown in cultured DOK and patient biopsies.[9,10] In fact, our more recent studies demonstrate that nuclear accumulation of β-catenin gradually augments from mild through moderate and severe dysplasia, and that these changes are associated with augmented Wnt3a in tissue biopsies.[12] Aside the requirement of Wnt ligands for nuclear accumulation of β-catenin in malignancy,[39,40] no information is available regarding molecular mechanisms involved in aberrant stabilization of β-catenin in premalignant lesions. Based on early evidence showing that endosomal sequestration of the destruction complex leads to stabilization and subsequent re-localization of β-catenin,[13,14,16,41] an intriguing possibility is that this process is upregulated in initial steps of carcinogenesis. Indeed, our observations indicated that endosomal localization of components of the destruction complex, including APC, Axin and GSK3β, is substantially increased in dysplasia, as shown in cell culture models and in clinical samples. Intriguingly, recent studies provide elegant examples connecting the β-catenin destruction complex, endosome trafficking and augmented Wnt/β-catenin signaling in malignancy. Specifically, whereas intact APC inhibits ligand-independent clathrin-mediated endocytosis, APC mutation in colorectal cancer allows augmented β-catenin signaling via increased endocytic trafficking.[42] Alternatively, increased vesicle acidification in colorectal cancer has been shown to promote APC degradation via the endolysosomal pathway, leading to enhanced β-catenin signaling.[43] Nevertheless, the roles of endosome trafficking and Wnt/β-catenin signaling in oral dysplasia remain unexplored, and hence, our findings showing that increased Rab5 activity, endosomal sequestration of the destruction complex, and nuclear localization of β-catenin, contribute to understanding the relevance of this mechanism in early oral lesions.

Although endosomal sequestration of the destruction complex has been extensively studied in non-tumor cells, the identity of molecular players controlling this phenomenon is not completely clear. The latter becomes intriguing, in the light that a subset of endosomal regulators—the Rabs—have gained attention for their role in different pathologies, including cancer.[17-21] Hence, the identification of Rab5 as a critical factor required for the recruitment of APC, GSK3β, and Axin within early endosomes, and consequently nuclear accumulation of β-catenin and transcription of target genes, is striking, since Rab5 is upregulated in cancer clinical samples, including lung adenocarcinoma,[22] pancreatic cancer,[23] ovarian cancer,[24] hepatocellular carcinoma,[25] and OSCC.[18] In addition, these findings raise the intriguing possibility that Rab5 activity is upregulated in early carcinogenesis, or even in potentially malignant lesions. Indeed, pull-down data supported this notion, since Rab5, but not other Rab proteins, including Rab7 or Rab11, underwent increased activation in DOK, further indicating that this phenomenon is not generalized for all Rabs.

The observations that Rab5 activity is higher in DOK, when compared with OKF6, raise the possibility that the endo-lysosomal system is deregulated in premalignant cells. Although this intriguing possibility is supported by immunofluorescence data showing changes in the population of

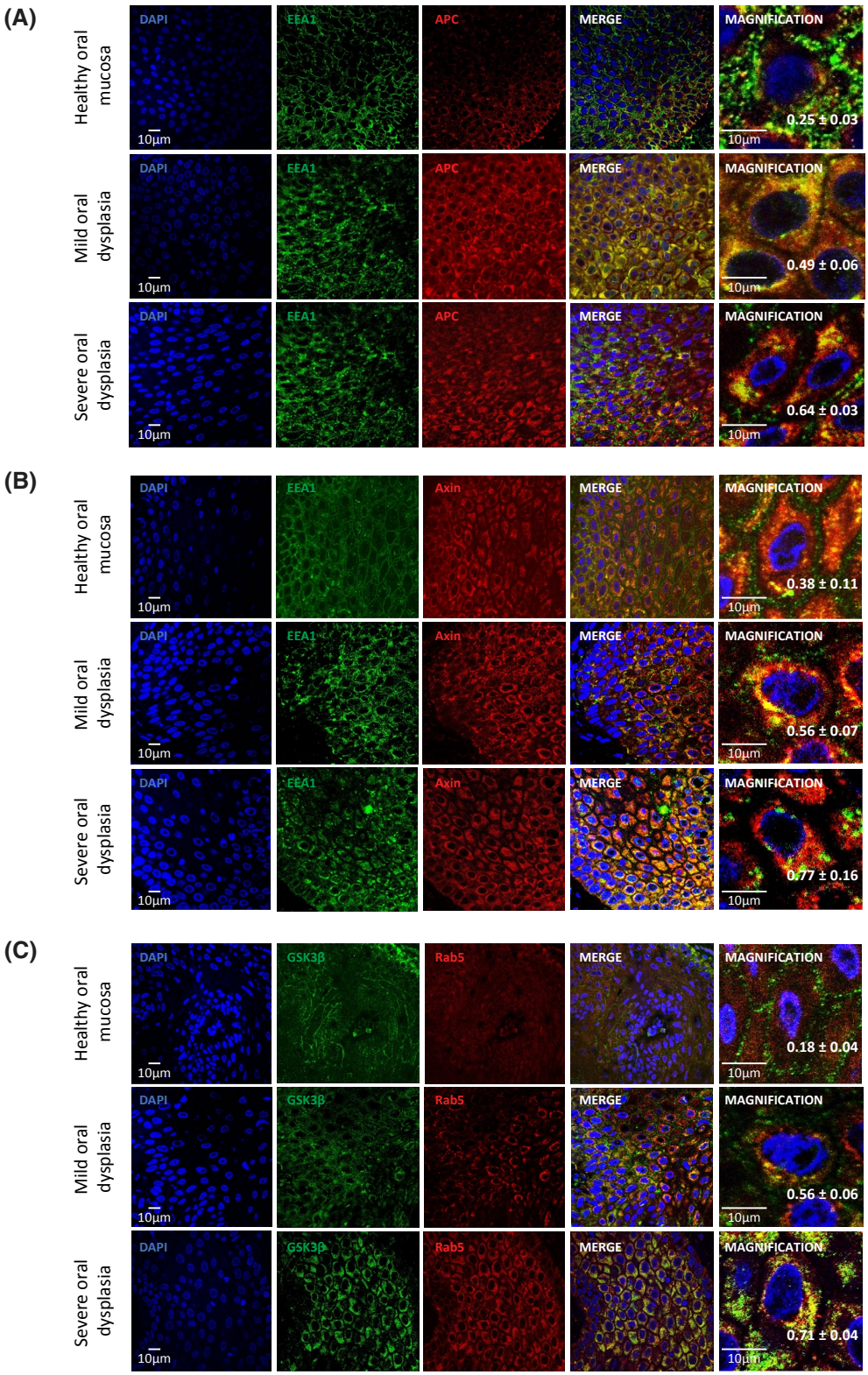

FIGURE 7 Endosomal localization of APC and Axin in oral dysplasia biopsies. Tissue immunofluorescence of Axin and EEA1 (A), APC and EEA1 (B) and GSK3β and Rab5 (C) was performed in healthy oral mucosa, mild and severe oral dysplasia biopsies. Nuclei were visualized with DAPI. Representative images are shown (bar represents 10 µm). Right panels correspond to magnifications of merged images. Numbers inside images indicate the Mander's Coefficient, obtained by averaging at least 50 cells per tissue (mean ± SD)

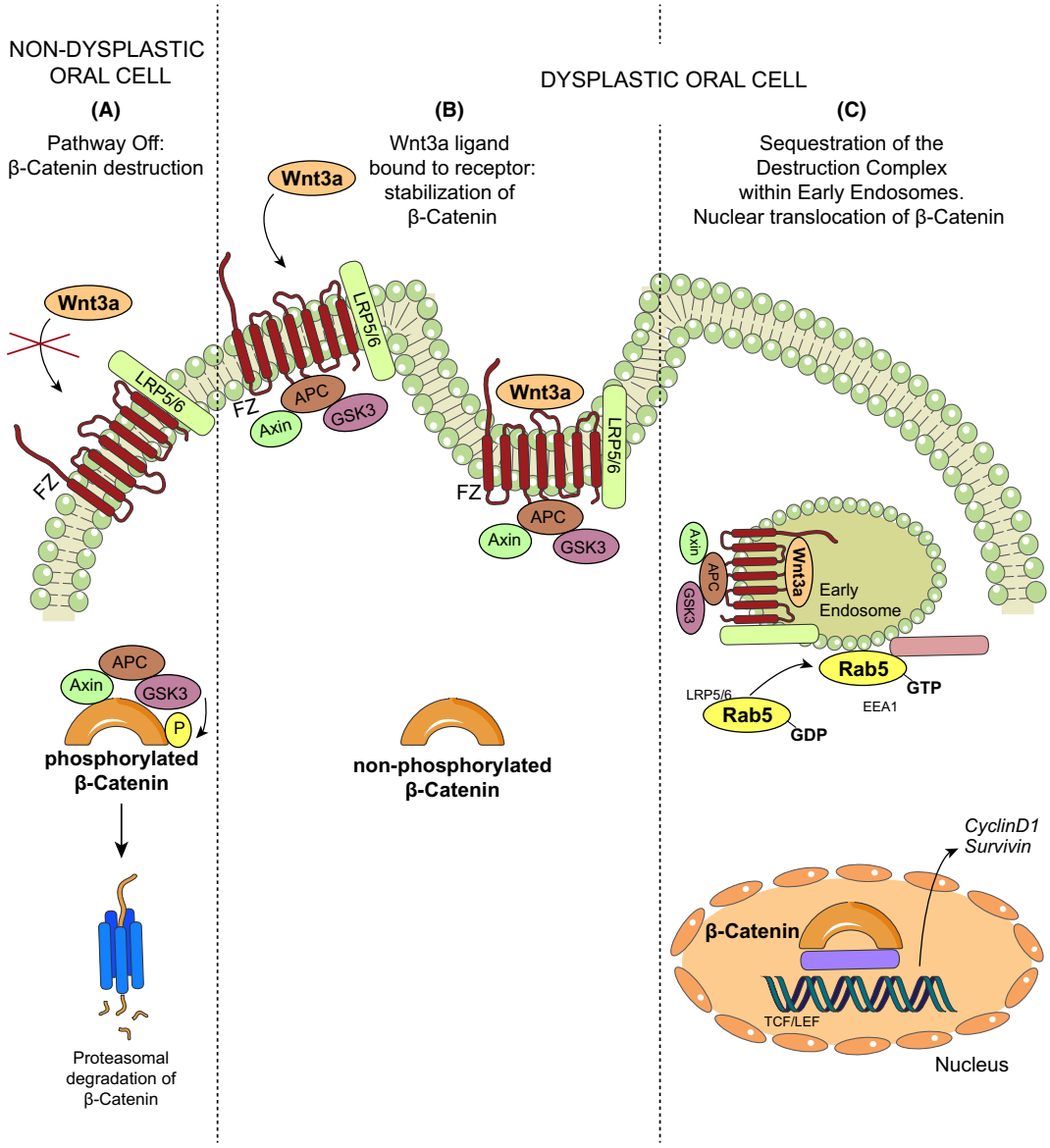

FIGURE 8 Proposed model for the upregulation of β-catenin signaling in oral dysplasia. A, In the absence of Wnt ligand, β-catenin is constitutively recruited by the destruction complex, formed by APC, Axin and GSK3β, among other components, phosphorylated by GSK3β and subsequently targeted for degradation via proteasome.[15] While most β-catenin is detected at cell-cell junctions, cytosolic and nuclear β-catenin levels remain negligible in OKF6. B,C, In oral dysplasia, nuclear β-catenin is substantially increased, due to several facts, including augmented secretion of Wnt3a (B)[12] and endosomal sequestration of the β-catenin destruction complex (C) (this study). Endosomal sequestration of the destruction complex allows β-catenin to stabilize and translocate to the nucleus, leading to the transcription of target genes upregulated in premalignant lesions. These events require activation of the endosomal protein Rab5, a small GTPase upregulated in oral dysplasia, since interference with Rab5 activity decreases endosomal sequestration of GSK3β, APC, and Axin, thereby preventing nuclear accumulation of β-catenin and transcription of target genes

Rab7- and Rab11-positive endosomes, conclusions should be carefully drawn, since additional studies need to be performed to support this notion, using additional markers for late and recycling endosomes, as well as appropriate tools to assess spatiotemporal fluctuations in GTP-bound Rab7 and Rab11. Noteworthy, increased early endosome number and size were observed in both cultured dysplastic cells and in sample biopsies, indicating that Rab5-dependent function at early endosomes is a feasible target in oral dysplasia. In fact, increased early endosome size may constitute an unanticipated, novel marker for diagnosis of premalignant lesions. However, further investigation is required to confirm such provoking possibility. In summary, this study shows for the first time that nuclear accumulation of β-catenin and the expression of target genes in oral dysplasia, is due to increased recruitment of the destruction complex within early endosomes, which is dependent on the activation of Rab5 (Figure 8, proposed model). Accordingly, the

activation status of Rab5 is identified as a novel molecular hit deregulated in oral dysplasia.

ACKNOWLEDGMENTS

This work was supported by the National Fund for Scientific and Technological Development (FONDECYT) 1180495 (to VAT); the Advanced Center for Chronic Diseases, FONDAP-ACCDiS 15130011 (to VAT); FONDECYT 1171075 (to AC); FONDECYT 3170660 (to PS); and a National Commission for Scientific and Technological Research (CONICYT) Fellowship (to MR).

CONFLICT OF INTEREST

The authors declare no conflicts of interest.

AUTHOR CONTRIBUTIONS

M. Reyes and V. Torres designed research, performed research, contributed with reagents and analytic tools, analyzed data and wrote the paper; D. Peña-Oyarzún performed research, analyzed data and reviewed the paper; P. Silva performed research and analyzed data; S. Venegas performed research and analyzed data; A. Criollo contributed with reagents and reviewed the paper.

REFERENCES

1. Dost F, Le Cao K, Ford PJ, Ades C, Farah CS. Malignant transformation of oral epithelial dysplasia: a real-world evaluation of histopathologic grading. *Oral Surg Oral Med Oral Pathol Oral Radiol*. 2014;117:343-352.
2. van der Waal I. Oral potentially malignant disorders: is malignant transformation predictable and preventable? *Med Oral Patol Oral Cir Bucal*. 2014;19:e386-e390.
3. Warnakulasuriya S, Johnson NW, van der Waal I. Nomenclature and classification of potentially malignant disorders of the oral mucosa. *J Oral Pathol Med*. 2007;36:575-580.
4. Warnakulasuriya S, Reibel J, Bouquot J, Dabelsteen E. Oral epithelial dysplasia classification systems: predictive value, utility, weaknesses and scope for improvement. *J Oral Pathol Med*. 2008;37:127-133.
5. Polanska H, Raudenska M, Gumulec J, et al. Clinical significance of head and neck squamous cell cancer biomarkers. *Oral Oncol*. 2014;50:168-177.
6. Speight PM. Update on oral epithelial dysplasia and progression to cancer. *Head Neck Pathol*. 2007;1:61-66.
7. Angiero F, Berenzi A, Benetti A, et al. Expression of p16, p53 and Ki-67 proteins in the progression of epithelial dysplasia of the oral cavity. *Anticancer Res*. 2008;28:2535-2539.
8. Gonzalez-Moles MA, Ruiz-Avila I, Gil-Montoya JA, Esteban F, Bravo M. Analysis of Ki-67 expression in oral squamous cell carcinoma: why Ki-67 is not a prognostic indicator. *Oral Oncol*. 2010;46:525-530.
9. Ishida K, Ito S, Wada N, et al. Nuclear localization of beta-catenin involved in precancerous change in oral leukoplakia. *Mol Cancer*. 2007;6:62.
10. Reyes M, Rojas-Alcayaga G, Maturana A, Aitken JP, Rojas C, Ortega AV. Increased nuclear beta-catenin expression in oral potentially malignant lesions: a marker of epithelial dysplasia. *Med Oral Patol Oral Cir Bucal*. 2015;20:e540-e546.
11. Sato K, Okazaki Y, Tonogi M, Tanaka Y, Yamane GY. Expression of beta-catenin in rat oral epithelial dysplasia induced by 4-nitroquinoline 1-oxide. *Oral Oncol*. 2002;38:772-778.
12. Reyes M, Pena-Oyarzun D, Maturana A, Torres VA. Nuclear localization of beta-catenin and expression of target genes are associated with increased Wnt secretion in oral dysplasia. *Oral Oncol*. 2019;94:58-67.
13. Taelman VF, Dobrowolski R, Plouhinec JL, et al. Wnt signaling requires sequestration of glycogen synthase kinase 3 inside multivesicular endosomes. *Cell*. 2010;143:1136-1148.
14. Yamamoto H, Komekado H, Kikuchi A. Caveolin is necessary for Wnt-3a-dependent internalization of LRP6 and accumulation of beta-catenin. *Dev Cell*. 2006;11:213-223.
15. Logan CY, Nusse R. The Wnt signaling pathway in development and disease. *Annu Rev Cell Dev Biol*. 2004;20:781-810.
16. Metcalfe C, Bienz M. Inhibition of GSK3 by Wnt signalling–two contrasting models. *J Cell Sci*. 2011;124:3537-3544.
17. Chia WJ, Tang BL. Emerging roles for Rab family GTPases in human cancer. *Biochim Biophys Acta*. 2009;1795:110-116.
18. da Silva SD, Marchi FA, Xu B, et al. Predominant Rab-GTPase amplicons contributing to oral squamous cell carcinoma progression to metastasis. *Oncotarget*. 2015;6:21950-21963.
19. Johnson IR, Parkinson-Lawrence EJ, Keegan H, et al. Endosomal gene expression: a new indicator for prostate cancer patient prognosis? *Oncotarget*. 2015;6:37919-37929.
20. Mosesson Y, Mills GB, Yarden Y. Derailed endocytosis: an emerging feature of cancer. *Nat Rev Cancer*. 2008;8:835-850.
21. Qin X, Wang J, Wang X, Liu F, Jiang B, Zhang Y. Targeting Rabs as a novel therapeutic strategy for cancer therapy. *Drug Discov Today*. 2017;22:1139-1147.
22. Yu L, Hui-chen F, Chen Y, et al. Differential expression of RAB5A in human lung adenocarcinoma cells with different metastasis potential. *Clin Exp Metastasis*. 1999;17:213-219.
23. Igarashi T, Araki K, Yokobori T, et al. Association of RAB5 overexpression in pancreatic cancer with cancer progression and poor prognosis via E-cadherin suppression. *Oncotarget*. 2017;8:12290-12300.
24. Zhao Z, Liu XF, Wu HC, et al. Rab5a overexpression promoting ovarian cancer cell proliferation may be associated with APPL1-related epidermal growth factor signaling pathway. *Cancer Sci*. 2010;101:1454-1462.
25. Fukui K, Tamura S, Wada A, et al. Expression of Rab5a in hepatocellular carcinoma: possible involvement in epidermal growth factor signaling. *Hepatol Res*. 2007;37:957-965.
26. Stenmark H. Rab GTPases as coordinators of vesicle traffic. *Nat Rev Mol Cell Biol*. 2009;10:513-525.
27. Frittoli E, Palamidessi A, Marighetti P, et al. A RAB5/RAB4 recycling circuitry induces a proteolytic invasive program and promotes tumor dissemination. *J Cell Biol*. 2014;206:307-328.
28. Mendoza P, Ortiz R, Diaz J, et al. Rab5 activation promotes focal adhesion disassembly, migration and invasiveness in tumor cells. *J Cell Sci*. 2013;126:3835-3847.
29. Palamidessi A, Frittoli E, Ducano N, et al. The GTPase-activating protein RN-tre controls focal adhesion turnover and cell migration. *Curr Biol*. 2013;23:2355-2364.
30. Silva P, Mendoza P, Rivas S, et al. Hypoxia promotes Rab5 activation, leading to tumor cell migration, invasion and metastasis. *Oncotarget*. 2016;7:29548-29562.

31. Silva P, Soto N, Diaz J, et al. Down-regulation of Rab5 decreases characteristics associated with maintenance of cell transformation. *Biochem Biophys Res Commun*. 2015;464:642-646.
32. Diaz J, Mendoza P, Ortiz R, et al. Rab5 is required in metastatic cancer cells for Caveolin-1-enhanced Rac1 activation, migration and invasion. *J Cell Sci*. 2014;127:2401-2406.
33. Luo J, Chen J, Deng ZL, et al. Wnt signaling and human diseases: what are the therapeutic implications? *Lab Invest*. 2007;87:97-103.
34. Reya T, Clevers H. Wnt signalling in stem cells and cancer. *Nature*. 2005;434:843-850.
35. Arriagada C, Silva P, Millet M, Solano L, Moraga C, Torres VA. Focal adhesion kinase-dependent activation of the early endocytic protein Rab5 is associated with cell migration. *J Biol Chem*. 2019;294:12836-12845.
36. Vanlandingham PA, Ceresa BP. Rab7 regulates late endocytic trafficking downstream of multivesicular body biogenesis and cargo sequestration. *J Biol Chem*. 2009;284:12110-12124.
37. Torres VA, Mielgo A, Barila D, Anderson DH, Stupack D. Caspase 8 promotes peripheral localization and activation of Rab5. *J Biol Chem*. 2008;283:36280-36289.
38. Cong F, Varmus H. Nuclear-cytoplasmic shuttling of Axin regulates subcellular localization of beta-catenin. *Proc Natl Acad Sci U S A*. 2004;101:2882-2887.
39. He S, Lu Y, Liu X, et al. Wnt3a: functions and implications in cancer. *Chin J Cancer*. 2015;34:554-562.
40. Prasad CP, Manchanda M, Mohapatra P, Andersson T. WNT5A as a therapeutic target in breast cancer. *Cancer Metastasis Rev*. 2018;37:767-778.
41. Blitzer JT, Nusse R. A critical role for endocytosis in Wnt signaling. *BMC Cell Biol*. 2006;7:28.
42. Saito-Diaz K, Benchabane H, Tiwari A, et al. APC inhibits ligand-independent Wnt signaling by the clathrin endocytic pathway. *Dev Cell*. 2018;44:566-581.e568.
43. Jung YS, Jun S, Kim MJ, et al. TMEM9 promotes intestinal tumorigenesis through vacuolar-ATPase-activated Wnt/beta-catenin signalling. *Nat Cell Biol*. 2018;20:1421-1433.

SUPPORTING INFORMATION

Additional supporting information may be found online in the Supporting Information section.

How to cite this article: Reyes M, Peña-Oyarzún D, Silva P, Venegas S, Criollo A, Torres VA. Nuclear accumulation of β-catenin is associated with endosomal sequestration of the destruction complex and increased activation of Rab5 in oral dysplasia. *The FASEB Journal*. 2020;34:4009–4025. https://doi.org/10.1096/fj.201902345RR